CrossMark

RESEARCH ARTICLE

Influence of environmental factors on absorption characteristics of suspended particulate matter and CDOM in Liaohe River watershed, northeast China

Tiantian Shao[1,2,3] · Hui Zheng[2] · Kaishan Song[3] · Ying Zhao[3] · Bai Zhang[3]

Abstract Absorption characteristics of optically active substances, including non-algal particles, phytoplankton, and chromophoric dissolved organic matter (CDOM), were measured in conjunction with environmental factors in five rivers within the Liaohe River watershed. Spectral absorption of non-algal particles $[a_{\mathrm{NAP}}(\lambda)]$ was similar to that of total particles for most samples, suggesting that the absorption of the total particles $[a_{\mathrm{p}}(\lambda)]$ was dominated by $a_{\mathrm{NAP}}(\lambda)$. The CDOM absorption spectra $[a_{\mathrm{CDOM}}(\lambda)]$ of West Liaohe and Taizihe rivers were easily distinguished from those of Hunhe, Liaohe, and East Liaohe rivers. Redundancy analysis indicated that absorption by optically active substances and anthropogenic nutrient disturbances probably resulted in the diversity of water quality parameters. The environmental variables including dissolved organic carbon, total alkalinity (TAlk), and total nitrogen (TN) had a significant correlation with CDOM absorption at 440 nm $[a_{\mathrm{CDOM}}(440)]$. There was almost no correlation between $a_{\mathrm{p}}(\lambda)$ and chlorophyll a, TN, total phosphorus, and TAlk. Moreover, total copper ion concentration and mercury ion concentration had a strong correlation with $a_{\mathrm{p}}(440)$, $a_{\mathrm{p}}(675)$, $a_{\mathrm{NAP}}(440)$, and $a_{\mathrm{NAP}}(675)$. The concentration of total aluminum ions exhibited a positive correlation with $a_{\mathrm{p}}(675)$ and $a_{\mathrm{NAP}}(675)$ ($p < 0.05$), and a significant correlation was observed between total arsenic concentration and $a_{\mathrm{CDOM}}(440)$. Furthermore, the interaction between metal ions and optically active substances provided an insight into particulates and CDOM properties linked to water quality characteristics for rivers in semiarid areas.

Keywords Liaohe River · Absorption characteristics · Particulates · CDOM · Heavy metals

✉ Kaishan Song
  songks1106@163.com

[1] Key Research Institute of Yellow River Civilization and Sustainable Development of Henan University, Kaifeng, Henan 475001, China

[2] College of Environment and Planning, Henan University, Kaifeng 475001, China

[3] Northeast Institute of Geography and Agroecology, Chinese Academy of Sciences, Key Laboratory of Wetland Ecology and Environment, Changchun 130102, China

Introduction

The absorption properties of chromophoric dissolved organic matter (CDOM) and suspended particulate matter (algal and non-algal particles) are the inherent optical properties (IOPs) of natural waters. The IOPs are the most significant factors affecting light propagation within water columns, and they play an important role in determining the underwater light climate and bio-optical algorithms for water quality assessment using remote sensing. As a result, the IOPs are critical parameters in radiative transfer models in a water column and bio-optical models for estimation of aquatic biomass and carbon pools (Tilstone et al. 2005; Zhang et al. 2007a; Li et al. 2013).

The total absorption of natural waters $[a(\lambda)]$ consists of absorption of CDOM $[a_{\mathrm{CDOM}}(\lambda)]$, phytoplankton $[a_{\mathrm{ph}}(\lambda)]$, non-algal particles $[a_{\mathrm{NAP}}(\lambda)]$, and pure water $[a_{\mathrm{w}}(\lambda)]$. As the pure water absorption at a given wavelength is constant, the absorption properties of IOPs, resulting in the attenuation of solar radiation in aquatic ecosystems, are determined by phytoplankton, non-algal particles, and CDOM. Previous studies have provided valuable evidence on the optical properties of suspended sediment in class II waters (Babin et al. 2003; Stramski et al. 2004; Binding et al. 2008). In general, particle size and composition

determine the optical behavior of suspended sediments, resulting in large variations of optical properties in the dynamic regions of coastal, river delta, and shelf seas (Binding et al. 2005; Long and Pavelsky 2013). Moreover, CDOM, as one of the major light-absorbing constituents in natural waters, absorbs the solar radiation in the ultraviolet and visible ranges and is largely responsible for the bio-optical properties of natural water (Organelli et al. 2014; Wen et al. 2016). In aquatic systems, phytoplankton competes with non-algal particles and CDOM for photosynthetically active radiation (PAR) (Vähätalo et al. 2005). Many studies have confirmed that the contribution of phytoplankton to the total absorption of PAR ranges from nearly zero to almost 100%, and the differences in the contributions of phytoplankton and CDOM will influence the maximum photosynthetic rate (Vähätalo et al. 2005; Zhang et al. 2007a; Kalenak et al. 2013).

Correlations between many water quality parameters (chlorophyll a [Chla], dissolved organic carbon [DOC], total suspended matter [TSM], total nitrogen [TN], total phosphorous [TP], and others) and a(λ) have been discussed in many previous studies (Gonnelli et al. 2013; Kitidis et al. 2006; Niu et al. 2014; Phong et al. 2014), while the other physicochemical parameters of water, such as heavy metal concentrations including arsenic (As), iron (Fe), and mercury (Hg), have also been investigated in different aquatic environments (Maloney et al. 2005; Schelker et al. 2011; Xiao et al. 2013). Generally, $a_{NAP}(\lambda)$ is closely correlated with TSM, inorganic suspended matter (ISM), and organic suspended matter (OSM), while significant positive correlations were found between $a_{ph}(\lambda)$ and Chla (Zhang et al. 2007a; Binding et al. 2008). Significant positive relationships between CDOM absorption and DOC have been found for most class I and class II waters (Zhang et al. 2007a; Del Castillo and Miller 2008; Fichot and Benner 2011; Spencer et al. 2012; Hestir et al. 2015; Shao et al. 2016). More importantly, the relationship between the absorption of CDOM and Chla concentration has received widespread attention because the strong absorption of CDOM in the blue spectral region interferes with the determination of Chla concentration by remote image sensing (Siegel et al. 2005; Zhang et al. 2009). Relationships between CDOM absorption at particular wavelengths and Chla concentrations were identified in Lake Taihu, the central eastern Mediterranean Basin (Zhang et al. 2007b; Bracchini et al. 2010), the NW Mediterranean Sea (Organelli et al. 2014), and in potable waters in northeast China (Shao et al. 2016). According to the previous studies, the distribution of heavy metal concentrations in water depends on the three kinds of water components, i.e., the suspended sediments, phytoplankton, and dissolved organic matter (DOM) (Chen et al. 2010). The absorption of CDOM in various waters has been shown to be associated with the concentrations of heavy metals. Studies published to date confirmed strong relationships between ions and CDOM in different study areas (Kalbitz and Wennrich 1998; Maloney et al. 2005; Schelker et al. 2011; Xiao et al.

2013; Gao et al. 2016). Total ferric ion concentration (TFe) was found to be strongly related to a_{CDOM}(320) in the 0–12-m-depth layer of a humic and mesotrophic lake (Lake Lacawac) and to DOC in Suwannee River (Maloney et al. 2005; Xiao et al. 2013). Numerous studies have shown strong positive relationships between total mercury ion concentration (THg) and DOC in stream water (Schuster et al. 2008; Selvendiran et al. 2008; Dittman et al. 2009; Schelker et al. 2011). The concentration of total chromium ion (TCr), THg, total copper ions (TCu), and total arsenic ions (TAs) in soil percolates was positively correlated with DOM, while initial DOM concentrations and dissolved arsenic concentrations showed a linear relationship for aquatic experiments (Kalbitz and Wennrich 1998; Anawar et al. 2003). However, compared with the number of studies on the relationship between DOM (DOC/CDOM) and heavy metals, fewer investigations are focused on the interaction between $a_{ph}(\lambda)$, $a_{NAP}(\lambda)$, and the metal ions (Estapa et al. 2012), although characterization of such interaction is critical for understanding the characteristics and sources of the main constituents responsible for optically active substance absorption.

The Liaohe River watershed (LHW) is located in a semihumid/semiarid temperate continental climate zone, has many heavy industry cities in northeast China, and thus provides a uniquely diverse mix of local environments that allow researchers to study nutrient status, IOPs and apparent optical properties (AOPs), and primary production of riverine waters. Rivers in LHW present a wide range of pollution severity: pollution is generally light in the main stream, moderate along the tributaries, but severe downstream from large urban areas and petroleum-processing facilities according to National Surface Water Quality Monthly Report of China in September 2013. Based on the previous studies and the special geographical environment of LHW, the objectives of this study were to (i) characterize spatial variations of the absorption coefficients of five rivers in LHW and (ii) determine the environmental factors influencing the absorption coefficients. Consequently, the present study will contribute to bio-optics and studies of water quality using remote sensing and help look into the interaction between optically active substances and heavy metals in rivers of LHW with unique climatic and hydrological conditions.

Materials and methods

Study area

The LHW located in the south of northeast China (116° 30′– 125° 47′ E, 38° 43′–45° N) (Fig. 1) is bounded in the north by Songhua River watershed and the south by Bohai Bay. The LHW drains an area of approximately 22.9×10^4 km^2 and consists of Jilin, Liaoning, and Hebei provinces and the
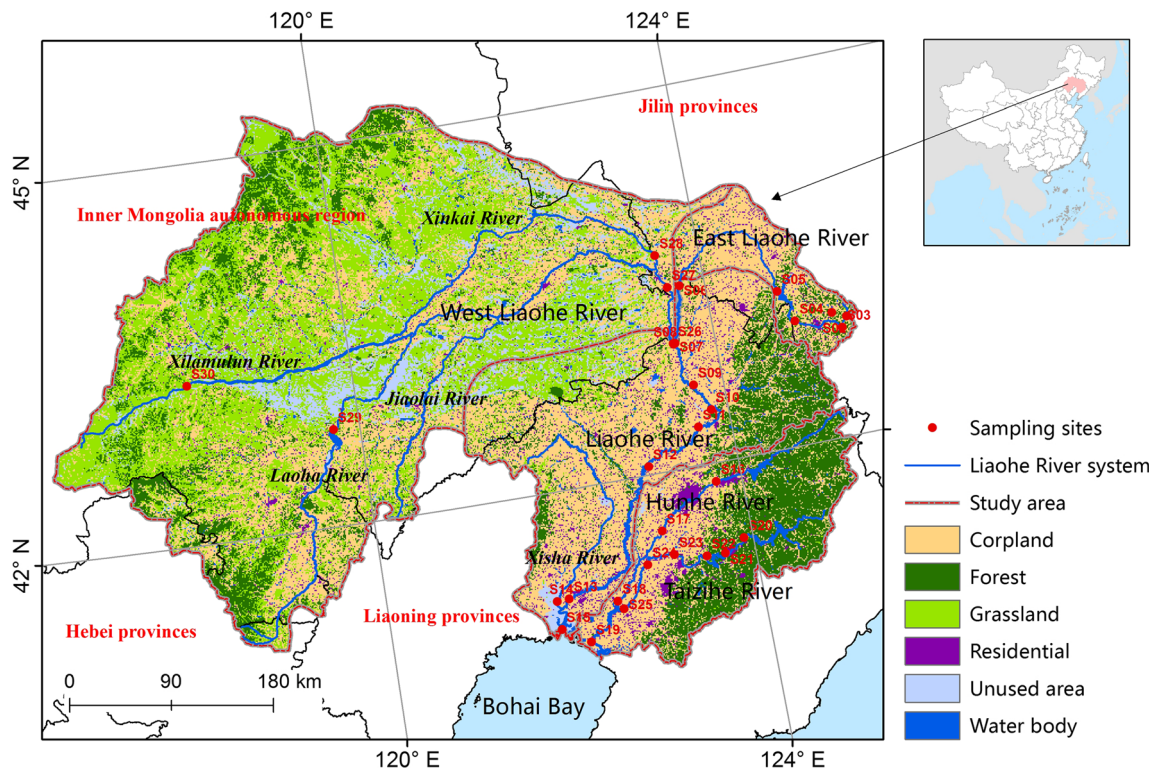
Fig. 1 Study area location and distribution of sampling sites

Inner Mongolia autonomous region. The Liaohe River system (LHRS) comprises two independent stream networks that flow in the approximate north–south direction and empty into the Bohai Sea. The first network encompasses the East and the West Liaohe rivers (Table 1). The West Liaohe River (WLR), including Xilamulun, Laoha, Xinkai, and Jiaolai rivers, is the largest tributary of the first river network, while the East Liaohe River (ELR) is the biggest tributary in the east of LRW. The second stream network, i.e., the Big Liaohe River, includes the Hunhe (HHR) and Taizihe (TZR) rivers as its main tributaries and empties into the Bohai Sea at Yingkou City (Table 1). The study area is located in a semihumid/semiarid temperate continental climate zone with the mean air temperature ranging between 4 and 7 °C and decreasing from south to north. Annual precipitation is slightly greater in the eastern than in the western sections of the LHW. Soil erosion is very serious particularly in some drought-prone areas in northeast China where vegetation coverage is less than 30%.

Sample collection

Surface water samples were collected approximately 0.1 m below the water surface at each sampling location which is generally located in the middle of the river. Two field campaigns resulted in a collection of 30 groups of data after elimination of repeated samples. The first one was conducted in late September 2013, and 28 groups of water samples (Fig. 1, S1–S28) were collected along the main trunk and the tributaries of the LHR including ELR, WLR, HHR, and TZR. The supplementary samples collected in early October including two samples at the ELR (S6, S7), five samples at the WLR (S26–S30), and two samples at the main stream of the Liaohe River after its junction with the East and West Liaohe rivers (S8, S9). Approximately a 2.5 L water sample was collected at each sampling site for determination of water physical and chemical parameters, e.g., Chla, TN, TP, DOC, and TSM concentrations. Water samples were collected in acid-washed HDPE bottles and held in thermoelectric coolers while in the

Table 1 Names of rivers, sampling numbers, drainage area, length, and maximum water depth for the samples collected in Liaohe River watershed

Name	Sampling number	Drainage area (km²)	Max depth (m)	Length (km)
East Liaohe River	S1–S7	11,450	0.9	383
Liaohe River	S8–S15	36,910	15.8	516
Hunhe River	S16–S19	36,061	6.2	415
Taizihe River	S20–S25		1.2	412
West Liaohe River	S26–S30	136,210	0.8	449

field. In the laboratory, these samples were kept in the dark at 4 °C until analyzing within 2 days.

Measurements of absorption coefficients

The values of $a_p(\lambda)$, $a_{NAP}(\lambda)$, and $a_{ph}(\lambda)$ were determined by the quantitative filter technique (QFT). Water samples were filtered through a 47-mm-diameter Whatman GF/F filter (0.7 μm), and absorption spectra were recorded every 1 nm from 350 to 800 nm using a Shimadzu UV-2600 PC UV-Vis spectrophotometer. A blank filter wetted with filtered water was used as a reference. In order to eliminate the differences between sample and reference filters, the optical density of 750 nm was subtracted from all measured spectra. The $a_p(\lambda)$ is expressed

$$a_p(\lambda) = 2.303 \times \frac{s}{v} ODS(\lambda) \qquad (1)$$

where 2.303 is the factor used to convert base 10 to natural logarithm, s is the filter clearance area, and v is the filtered volume of samples.

After each measurement of the optical densities of the total particles, the filter was soaked in 0.1% sodium hypochlorite. Algal particles were dissolved in sodium hypochlorite leaving non-algal particles on the filter. After rinsed with filtered water, the filters were then measured again to obtain the optical densities of the non-algal particles. $a_{NAP}(\lambda)$ was also calculated using Eq. (1), and $a_{ph}(\lambda)$ was obtained based on $a_p(\lambda)$ and $a_{NAP}(\lambda)$ as shown in Eq. (2):

$$a_{ph}(\lambda) = a_p(\lambda) - a_{NAP}(\lambda) \qquad (2)$$

The collected samples were filtered through a precombusted Whatman GF/F filter (0.7 μm) at low pressure for measurement of the absorption coefficient of CDOM. Absorption spectra were measured between 200 and 800 nm at 1-nm intervals using a Shimadzu UV-2600 PC UV-Vis dual-beam spectrophotometer with a 1-cm quartz cuvette. Milli-Q water was used in the reference cuvette for CDOM absorption measurements. Absorption coefficients of CDOM were calculated as

$$a_{CDOM}\left(\lambda'\right) = 2.303 OD(\lambda)/l \qquad (3)$$

where $a_{CDOM}(\lambda')$ is the uncorrected CDOM absorption coefficient at wavelength λ, $OD(\lambda)$ is the optical density at the same wavelength, and l is the cuvette path length in meters. Because of the influence of backscattering by small particles and colloids that pass through filters, absorption coefficients are corrected based on the following equation (Bricaud et al. 1981):

$$a_{CDOM}(\lambda) = a_{CDOM}\left(\lambda'\right) - a_{CDOM}\left(750'\right)(\lambda/750) \qquad (4)$$

where $a_{CDOM}(\lambda)$ is the absorption coefficient at wavelength λ corrected for scattering and baseline fluctuations and $a_{CDOM}(\lambda')$ is the uncorrected absorption coefficient at a given λ.

Measurements of other parameters

TSM and ISM were determined by gravimetrical analysis (Song et al. 2012). By subtracting ISM from TSM, OSM was obtained. Concentrations of DOC, TN, and TP were measured according to Song et al. (2013). Chla was extracted using 90% acetone and measured with a Shimadzu UV-2600 PC spectrophotometer (Song et al. 2013). Concentrations of total metal ions (THg, TFe, TAs, etc.) were measured based on the GB3838-2002 (national quality standards for surface waters, China).

Spectral slope (S) determination

The spectral slope of $a_{CDOM}(\lambda)$ (S_g) was calculated by fitting exponential functions to the absorption spectrum in the ranges of 300 to 500 nm using the following equation (Zhang et al. 2007b; Spencer et al. 2012):

$$a_{CDOM}(\lambda) = a_{CDOM}(\lambda_0) \exp\left[S_g(\lambda_0 - \lambda)\right] \qquad (5)$$

where $a_{CDOM}(\lambda)$ is the CDOM absorption at a given wavelength, $a_{CDOM}(\lambda_0)$ is the absorption estimate at the reference wavelength λ_0, which is generally selected to be 440 nm, and S_g is the spectral slope fitting parameter.

Similarly, the spectral slope of $a_{NAP}(\lambda)$ (S_d) was also calculated with non-linear fit of an exponential function, shown as below:

$$a_d(\lambda) = a_d(\lambda_0) \exp[S_d(\lambda_0 - \lambda)] \qquad (6)$$

where $a_{NAP}(\lambda_0)$ is the absorption at the reference wavelength λ_0, which is generally selected to be 440 nm, and S_d is the spectral slope fitting parameter.

Least square regression was used to construct the absorption model of $a_{NAP}(\lambda)$ from 400 to 700 nm in order to compare with the results obtained from the other studies.

Statistical analysis

The absorption coefficients of optically active substances were calculated using Origin 8.0 software. Correlations between environmental parameters and the absorption of optically active substances were determined by redundancy analysis (RDA) using CANOCO 4.5, in which optically active substance absorptions were defined as species variables, and environmental parameters were selected as explanatory variables. Before RDA is conducted, detrended correspondence analysis (DCA) should be executed first, because the positions of the samples on the

second axis are strongly dependent on their positions on the first axis, and this effect can be interpreted as a limitation of the method (Lepš and Šmilauer 2003). As a result, DCA was used to remove this limitation. If the maximum lengths of gradient were smaller than 3, then RDA could be used with those data. A Monte Carlo permutation test was also conducted with CANOCO 4.5 to select environmental variables closely related to response variables (499 permutations under the reduced model, $p < 0.05$). The Pearson correlation coefficient (r) was calculated using SPSS 17.0.

Results

Light absorption by particles, CDOM, and phytoplankton

Particle absorption

The absorption coefficients of total suspended particles typically decreased monotonically with increasing wavelength (Fig. 2), suggesting that non-algal particles dominated the total particles. Rivers, where the flowing water entrains suspended sediments, have $a_p(\lambda)$ curves very similar to $a_{NAP}(\lambda)$. This situation always happens in rivers, estuaries, coastal zones, and other class II water bodies with high concentrations of inorganic particles (Binding et al. 2008). However, the absorption curves of samples from different rivers varied greatly. An inconspicuous absorption peak was present near 675 nm for most sites attributable to phytoplankton, but another absorption peak near 440 nm found in previous articles was not detected in samples from the LHW. In general, $a_p(\lambda)$ in ELR and LHR was higher than in other rivers, while TZR showed the lowest absorption coefficient. Large variation in $a_p(\lambda)$ along the ELR is shown in Fig. 2a and Table 2. For samples from HHR, $a_p(440)$ and $a_p(675)$ were lower than in samples from ELR. Likewise, $a_p(440)$ for LHR also exhibited a large variation, while $a_p(675)$ was relatively stable and much larger than in the other rivers investigated (Fig. 2b, Table 2). The average value for $a_p(440)$ in TZR was higher than in WLR, while the average value for $a_p(675)$ was lower in TZR than in WLR.

Non-algal particle absorption

Absorption characteristics of non-algal particles were determined by mineral particles and organic matter including the non-active organisms and non-algal active organisms (Binding et al. 2008). The absorption coefficient of non-algal particles decreased with increasing wavelength in all rivers (Fig. 2c). The $a_{NAP}(440)$ in ELR was a little higher than in HHR (Table 2). Considering the low $a_p(\lambda)$ in TZR and WLR, $a_{NAP}(440)$ in the two rivers also showed low values, with mean values of 1.25 and 4.23 m^{-1}, respectively.

As one of the most important bands in ocean color remote sensing, 440 nm was selected to build the absorption models of non-algal particle using the least square method. S_d in the wavelength range 400–700 nm in the present study was relatively stable from 9.97 m^{-1} for WLR to 13.06 m^{-1} for ELR, with a mean value of 11.41 m^{-1}. However, S_d varied in different rivers (Table 3). The mean S_d of HHR was higher than in the other rivers, while it was lowest in WLR. The coefficient of variation (CV), defined as the percentage of the ratio between standard deviation and the mean value, can be used to compare differences in samples from the same river. The CV in LHR was lower than in the other rivers, suggesting that the S_d of samples in LHR was similar to each other.

Phytoplankton absorption

Phytoplankton absorption varied with chlorophyll concentrations, which were influenced by the abundance and community composition of the phytoplankton community. The absorption spectra of phytoplankton showed that the pigments had two diagnostic absorption peaks: in the blue (approximately 440 nm) and red (approximately 675 nm) sections of the spectrum (Fig. 2e). The peak at 675 nm was determined by Chla, while the peak at 440 nm was affected simultaneously by Chla and the other accessory pigments (Zhang et al. 2007a).

The ratio between absorption at the blue and red wavelengths, $a_{ph}(440)/a_{ph}(675)$, can be used to distinguish Chla and auxiliary pigments. In the present study, $a_{ph}(440)/a_{ph}(675)$ of samples from HHR and LHR exhibited higher values (3.54 and 3.32, respectively) than those of the other rivers (1.73, 1.50, and 1.24 for ELR, TZR, and WLR, respectively), suggesting various compositions of phytoplankton in the different rivers.

CDOM absorption

The absorption of CDOM was similar to that of non-algal particles (Fig. 2). It was not difficult to distinguish $a_{CDOM}(\lambda)$ of WLR and TZR from those of HHR, LHR, and ELR. CDOM is often characterized using the absorption coefficient at specific wavelengths such as 254, 350, 355, and 440 nm (Ma et al. 2006; Zhang et al. 2007b; Spencer et al. 2012; Shen et al. 2012; Wang et al. 2014). In this study, the absorption of CDOM at 440 nm was used for comparative purposes. Obviously, $a_{CDOM}(440)$ in WLR was higher than in the other rivers, while TZR was the lowest with a mean value of 0.52 m^{-1} (Table 2).

Least squares regression was used to construct the absorption model of $a_{CDOM}(\lambda)$ with three different ranges including 275–295, 280–400, and 350–400 nm (Fig. 3). S_g values mainly depended on the range of wavelengths selected. The values of $S_{275–295}$ in all sites were a bit larger than those of $S_{280–400}$, and the values of $S_{350–400}$ were lower than those of $S_{280–400}$,

Fig. 2 Absorption spectrums of total suspended particles [$a_p(\lambda)$], non-algal particles [$a_{NAP}(\lambda)$], phytoplankton [$a_{ph}(\lambda)$], and chromophoric dissolved organic matter (CDOM) [$a_{CDOM}(\lambda)$] of sampling sites in different rivers
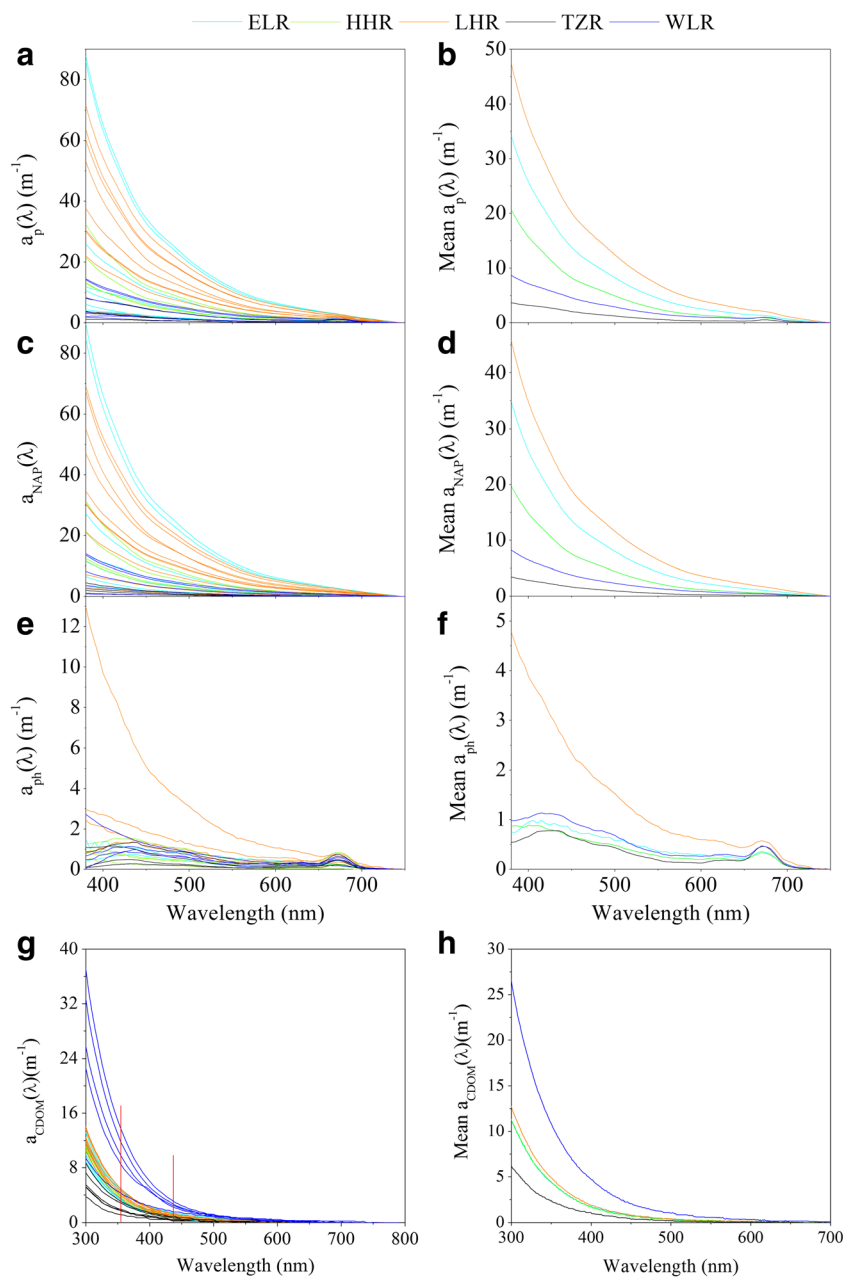
suggesting that S_g values decreased with increasing wavelength range. S_g values in the same river showed significant variation in ELR, TZR, and WLR but were relatively stable in HHR and LHR, relatively. The mean values of S_g based on different wavelength ranges were different from those of other water bodies. Mean values of $S_{350–400}$ in LHW were slightly higher than those of Changjiang River reported by Chen et al. (2013) and Elizabeth River with 0.0149 nm^{-1} (Helms et al. 2008), but they were lower than those in most rivers in the USA and the Yukon River (Spencer et al. 2009). Mean values of $S_{280–400}$ obtained in this study were higher than those in the Suwannee River (Xiao et al. 2013) but lower than those in

terminal lakes (Zhang et al. 2005). As a result, the molecular weight of CDOM composition in the LHW was higher than that of the Changjiang, Suwannee, and Elizabeth rivers, while it was lower than Yukon River located at high latitude. The slope ratio (S_R) of $S_{275–295}/S_{350–400}$ has also been calculated to characterize CDOM in natural waters, with lower relative values indicative of DOM of higher molecular weight, greater aromaticity, and increasing vascular plant inputs (Helms et al. 2008; Osburn et al. 2011). S_R values were greater than 1 except in one sample at TZR (Fig. 3), which was slightly higher than that obtained for most rivers in the USA, suggesting low molecular weight of CDOM in the LHW.

Table 2 Statistics of absorption of suspended particulate matter [$a_p(\lambda)$], non-algal particles [$a_{NAP}(\lambda)$], phytoplankton [$a_{ph}(\lambda)$], and chromophoric dissolved organic matter (CDOM) [$a_{CDOM}(\lambda)$]

Rivers	Statistics	Wavelength (nm)	Min–max (m^{-1})	Mean (m^{-1})
ELR	$a_p(\lambda)$ (m^{-1})	440	2.74–39.65	15.6 (±16.24)
		675	0.19–2.84	1.31 (±1.08)
	$a_{NAP}(\lambda)$ (m^{-1})	440	2.11–39.93	15.35 (±16.18)
		675	0.13–2.65	1.00 (±1.09)
	$a_{ph}(\lambda)$ (m^{-1})	440	0.62–0.93	0.76 (±0.16)
		675	0.27–0.58	0.43 (±0.16)
	$a_{CDOM}(\lambda)$ (m^{-1})	440	0.69–1.38	0.92 (±0.32)
HHR	$a_p(\lambda)$ (m^{-1})	440	6.53–14.47	9.38 (±3.67)
		675	0.56–1.32	0.89 (±0.34)
	$a_{NAP}(\lambda)$ (m^{-1})	440	5.39–13.91	8.62 (±3.94)
		675	0.41–0.81	0.55 (±0.18)
	$a_{ph}(\lambda)$ (m^{-1})	440	0.30–1.50	0.76 (±0.52)
		675	0.04–0.86	0.34 (±0.36)
	$a_{CDOM}(\lambda)$ (m^{-1})	440	0.92–0.92	0.92 (±0.00)
LHR	$a_p(\lambda)$ (m^{-1})	440	12.04–34.12	22.63 (±7.84)
		675	1.66–2.80	2.05 (±0.42)
	$a_{NAP}(\lambda)$ (m^{-1})	440	10.72–32.48	21.27 (±7.72)
		675	0.86–2.44	1.62 (±0.50)
	$a_{ph}(\lambda)$ (m^{-1})	440	0.45–5.91	2.00 (±2.02)
		675	0.28–0.82	0.51 (±0.19)
	$a_{CDOM}(\lambda)$ (m^{-1})	440	0.69–1.25	0.99 (±0.19)
TZR	$a_p(\lambda)$ (m^{-1})	440	0.87–5.49	2.35 (±1.66)
		675	0.16–1.30	0.52 (±0.43)
	$a_{NAP}(\lambda)$ (m^{-1})	440	0.59–4.14	1.86 (±1.25)
		675	0.05–0.55	0.18 (±0.19)
	$a_{ph}(\lambda)$ (m^{-1})	440	0.04–1.34	0.62 (±0.53)
		675	0.09–0.75	0.40 (±0.25)
	$a_{CDOM}(\lambda)$ (m^{-1})	440	0.23–0.92	0.52 (±0.25)
WLR	$a_p(\lambda)$ (m^{-1})	440	1.96–8.33	5.12 (±3.10)
		675	0.22–1.30	0.97 (±0.43)
	$a_{NAP}(\lambda)$ (m^{-1})	440	0.54–7.45	4.23 (±3.01)
		675	0.04–0.71	0.41 (±0.30)
	$a_{ph}(\lambda)$ (m^{-1})	440	0.07–1.41	0.89 (±0.50)
		675	0.18–0.96	0.56 (±0.28)
	$a_{CDOM}(\lambda)$ (m^{-1})	440	1.57–3.09	2.44 (±0.57)

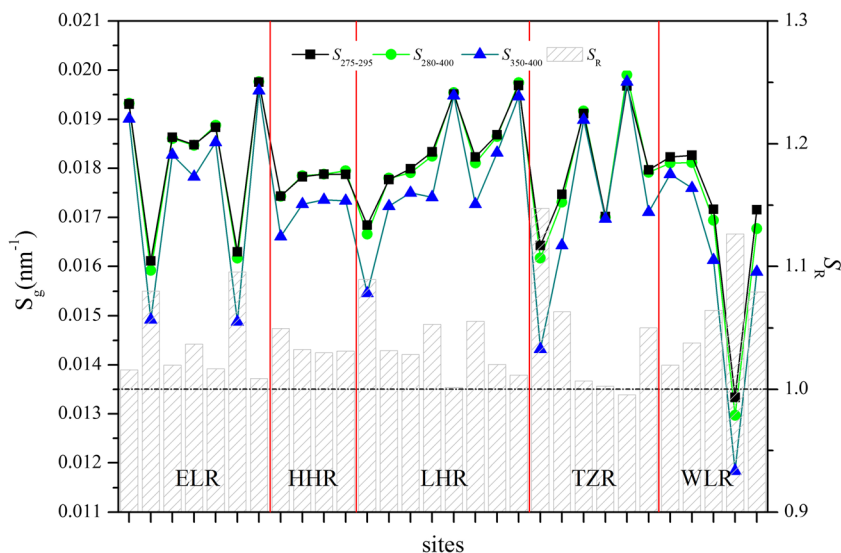## Contribution of non-algal particles, phytoplankton, and CDOM to the total absorption

The relative contribution of the different components to the total average absorption of all samples is shown in Fig. 4a, demonstrating that non-algal particles contributed the most to the total absorption from 380 to 650 nm. The CDOM contributed primarily to total absorption at short wavelengths, with a maximum at 380 nm for wavelengths 380–700 nm, and decreased with increasing wavelength; the absorption of CDOM was generally higher than that of phytoplankton at wavelengths shorter than 430 nm. The contribution of phytoplankton increased with increasing wavelength from 380 to 675 nm,

Table 3 Statistical parameters of S_d in different rivers

Rivers	Min	Max	Mean	CV	Fitting precision (r^2)
ELR	11.45	13.06	11.94	4.50%	0.96
HHR	11.83	12.56	12.32	2.74%	0.94
LHR	10.28	11.92	10.94	4.96%	0.94
TZR	11.21	12.11	11.72	4.11%	0.99
WLR	9.97	10.77	10.33	3.54%	0.98

S_d spectral slope of non-algal particle absorption, CV coefficient of variation

Fig. 3 Spatial variation of $S_{275–295}$, $S_{280–320}$, $S_{350–400}$, and S_R ($S_{275–295}/S_{350–400}$) in different rivers

appearing to peak near 675 nm, and decreased sharply from 675 to 700 nm.

The contributions of CDOM, phytoplankton, and non-algal particles at 440 nm in the five rivers are shown in Fig. 4b. Because of the constant and limited value at 440 nm (0.00635 m^{-1}), the absorption of pure water at 440 nm was ignored. According to Fig. 4b, 86.67% of absorption of all samples was associated with non-algal particles except in four samples from TZR and WLR. When compared with the predominant absorption of non-algal particles in most sites, only one sample in WLR showed that CDOM contributed most to the total absorption at 440 nm and absorption of only one sample at TZR was mainly driven by phytoplankton.

Correlations between environmental factors and light absorption

The collected river samples exhibited large variation in water quality (Table 4). TN and TCr concentrations exceeded the GB3838-2002 standard for class V waters of 2.0 mg N/L and 0.001 mg/L, respectively. Considering the lack of heavy metals obtained in two sites of WLR (Table 4), we grouped water quality parameters into general parameters and heavy metals.

General parameters

For the maximum gradient lengths based on DCA of 2.01 in this study, RDA was performed for all sampling locations with eight general water environmental variables. The RDA data showed that the forward selected explanatory variables could explain the variability of optically active substance characteristics with species–environment correlations of 0.805. The first two axes of RDA explained 96.3% of total variability in the absorption characteristics of all the water samples

collected (axis 1, 89.6%; axis 2, 6.7%). Coefficients between environmental variables with axes in RDA indicated that TSM, OSM, and ISM had strong correlations with $a_p(440)$ and $a_p(675)$ ($p < 0.01$, Table 5), while DOC had weak correlations with particle absorption. However almost no correlation was observed between the absorption of total suspended particles and Chla, TN, TP, and TAlk (Fig. 5a).

Correlations between non-algal absorption and water quality parameters were similar to the relationships between particle absorption and water quality parameters because of strong positive correlations between $a_{NAP}(440)$ and suspended particles (TSM, OSM, and ISM) and insignificant correlations between $a_{NAP}(440)$ and other parameters (Fig. 5a, Table 5). Moreover, $a_{NAP}(440)$ was highly correlated with OSM, followed by ISM and TSM. Non-algal particles include both organic and inorganic particles, and most of the organic particles are relict bodies and degraded products of phytoplankton (Binding et al. 2008). The high correlation between $a_{NAP}(440)$ and OSM suggests that non-algal particles accounted for a large percentage of OSM. However, there was no correlation between algal absorption and Chla (Table 5) for all samples. In addition, samples located in different rivers were analyzed separately, yet no significant correlation was obtained even though the samples belonged to different sub-watersheds.

Strong positive correlations between CDOM absorption coefficients and TN ($p < 0.05$), TAlk ($p < 0.01$), and DOC concentrations ($p < 0.01$) in all water samples were obtained in the LHW (Fig. 5a, Table 5). Weak correlations were obtained between suspended particles and CDOM absorption (Table 5). If samples located in different rivers were analyzed separately, not every river showed strong correlations between CDOM and DOC (Fig. 6), even though a very strong correlation was obtained between the two parameters for all the samples
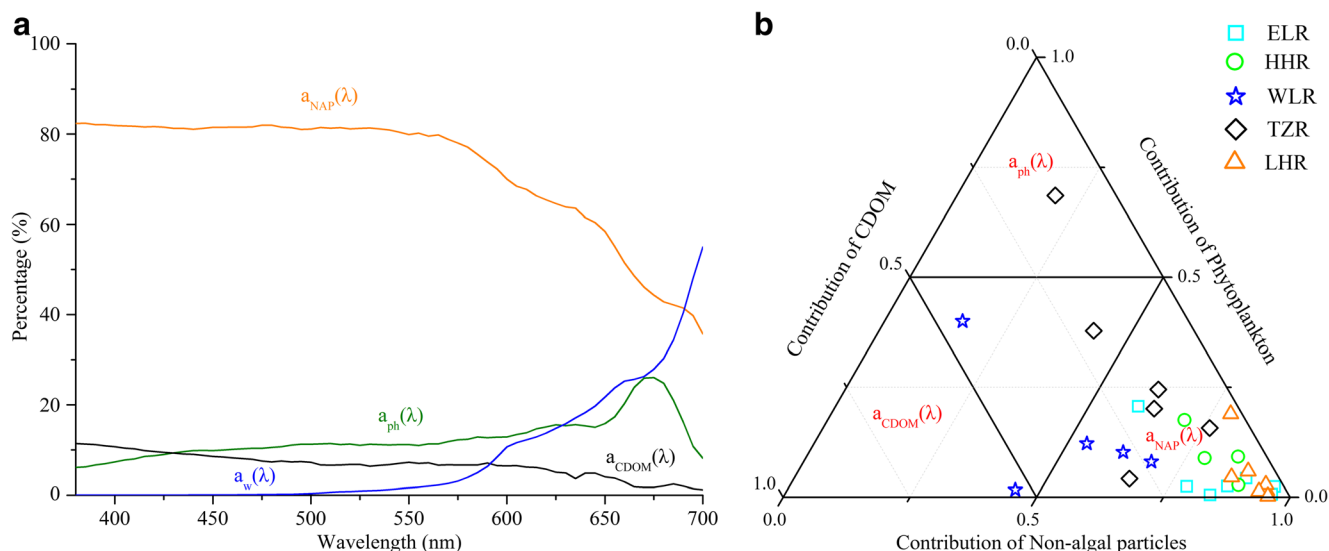
Fig. 4 Relative contribution of the absorption coefficients of pure water [$a_w(\lambda)$], $a_{CDOM}(\lambda)$, $a_{ph}(\lambda)$, and $a_{NAP}(\lambda)$ to the total absorption coefficient $a(\lambda)$ for the mean of samples from five rivers (**a**). Contribution of $a_{CDOM}(\lambda)$, $a_{ph}(\lambda)$, and $a_d(\lambda)$ at 440 nm in different rivers (**b**)

(Table 4). Considering the consistent $a_{CDOM}(440)$ obtained for HHR (Table 2), the relationship between CDOM and DOC for this river was consequently excluded from further analysis (Fig. 6). Significant correlations between $a_{CDOM}(440)$ and DOC were found in TZR ($r = 0.928$, $p < 0.01$) and WLR ($r = 0.872$, $p < 0.05$), while positive correlations were observed for ELR and LHR, with r values of 0.436 and 0.565, respectively. The r value between $a_{CDOM}(440)$ and TAlk indicated that CDOM absorption showed a positive correlation with TAlk in ELR and TZR, but had no correlation in LHR and WLR, which is inconsistent with the result for the samples analyzed together.

Metal ions

Six metal ions and the absorption of optically active substances in water samples were analyzed based on RDA (Fig. 5b). Because of the lack of data on metal ions in Xilamulun and Laoha rivers, 28 groups of data were used to study the correlations. The first two axes of RDA explained 73.5% of total variability in light absorption characteristics of all the water samples collected (axis 1, 70.7%; axis 2, 2.8%). The r values between the absorption of optically active substances and concentrations of metal ions are shown in Table 6. Several metal ions, including TAl, TFe, THg, and TCu,

Table 4 Water quality parameters of water samples collected in the Liaohe River watershed

| Water quality	ELR ($n = 7$)	HHR ($n = 4$)	LHR ($n = 8$)	TZR ($n = 6$)	WLR ($n = 5$)	GB3838-2002
DOC	10.71 ± 4.32	7.71 ± 0.89	3.77 ± 4.51	6.49 ± 1.49	14.20 ± 16.39	–
Chla	19.24 ± 17.23	22.95 ± 26.56	8.68 ± 14.14	27.08 ± 26.16	7.22 ± 9.21	–
TSM	312.17 ± 423.07	78.67 ± 22.50	196.86 ± 229.14	25.79 ± 23.52	126.84 ± 186.45	–
OSM	26.25 ± 31.55	13 ± 2.58	13.54 ± 15.59	4.14 ± 1.81	9.91 ± 11.52	–
ISM	285.92 ± 391.56	65.67 ± 21.05	183.32 ± 213.99	21.66 ± 22.57	122.54 ± 178.86	–
TN	3.64 ± 1.48	6.16 ± 0.53	0.79 ± 1.27	5.21 ± 1.68	0.32 ± 0.47	V (1.5–2.0)
TP	0.147 ± 0.057	0.21 ± 0.05	0.017 ± 0.022	0.12 ± 0.079	0.059 ± 0.071	II (0.1–0.2)
TAlk	109.71 ± 30.54	109.2 ± 9.90	187.2 ± 14.11	116.8 ± 32.08	56.83 ± 69.36	–
TAl	1.986 ± 0.42	2.60 ± 0.29	0.88 ± 1.05	1.24 ± 0.065	*0.43 ± 0.57*	–
TFe	0.661 ± 0.189	1.16 ± 0.15	0.52 ± 0.63	0.17 ± 0.10	*0.26 ± 0.37*	–
TCr	0.102 ± 0.008	0.0084 ± 0.0047	0.005 ± 0.006	0.004 ± 0.001	*0.007 ± 0.001*	V (0.005–0.01)
TCu	0.011 ± 0.022	0.0037 ± 0.0027	0.038 ± 0.061	0.002 ± 0.001	*0.017 ± 0.022*	I (<0.01)
TAs	0.037 ± 0.008	0.045 ± 0.011	0.006 ± 0.008	0.038 ± 0.011	*0.016 ± 0.022*	I (<50 μg/L)
THg	0.023 ± 0.009	0.12 ± 0.007	0.013 ± 0.014	0.019 ± 0.006	*0.003 ± 0.004*	I (<5 μg/L)

TAlk represents total alkalinity. The unit of absorption coefficients is m^{-1}. The unit of DOC, TSM, OSM, ISM, TN, and TP is mg/L, and the unit of Chla is μg/L. The unit of absorption coefficients is m^{-1}; the unit of TAl, TFe, TCu, and TCr is mg/L, and the unit of TAs and THg is μg/L. Concentrations of heavy metals in WLR, italic in the table, are the mean of three samples for the missing of data of Xilamulun and Laoha rivers

Table 5 Correlations between absorption and component concentrations

Parameters	$a_p(440)$	$a_p(675)$	$a_{NAP}(440)$	$a_{NAP}(675)$	$a_{ph}(440)$	$a_{ph}(675)$	$a_{CDOM}(440)$	DOC	Chla	TSM	OSM	ISM	TN	TP	TAlk
$a_p(440)$	1														
$a_p(675)$	0.871**	1													
$a_{NAP}(440)$	0.996**	0.851**	1												
$a_{NAP}(675)$	0.989**	0.887**	0.986**	1											
$a_{ph}(440)$	0.304	0.443*	0.217	0.289	1										
$a_{ph}(675)$	−0.223	0.264	−0.260	−0.212	0.334	1									
$a_{CDOM}(440)$	0.022	0.141	0.016	0.076	0.073	0.140	1								
DOC	0.171	0.334	0.148	0.223	0.282	0.240	0.887**	1							
Chla	−0.285	−0.184	−0.296	−0.275	0.040	0.185	0.037	−0.062	1						
TSM	0.783**	0.741**	0.782**	0.795**	0.217	−0.092	0.089	0.208	−0.330	1					
OSM	0.795**	0.750**	0.793**	0.814**	0.229	−0.114	0.141	0.256	−0.263	0.970**	1				
ISM	0.780**	0.739**	0.779**	0.792**	0.216	−0.090	0.084	0.203	−0.335	1.000**	0.965**	1			
TN	0.040	−0.166	0.016	0.002	0.263	−0.354	−0.386*	−0.443*	0.362*	−0.055	−0.008	−0.059	1		
TP	−0.069	−0.129	−0.081	−0.058	0.102	−0.153	0.360	0.214	0.414*	−0.175	−0.071	−0.183	0.406*	1	
TAlk	−0.072	0.237	−0.095	−0.005	0.232	0.513**	0.703**	0.813**	−0.088	0.080	0.073	0.080	−0.472**	0.095	1

TAlk represents total alkalinity. The unit of absorption coefficients is m^{-1}. The unit of DOC, TSM, OSM, ISM, TN, and TP is mg/L. The unit of Chla is μg/L

**Correlation is significant at the 0.01 level (two-tailed); *correlation is significant at the 0.05 level (two-tailed)

Fig. 5 Redundancy analysis (RDA) of absorption coefficients of optically active substances and (**a**) general water quality parameters ($n = 30$); **b** metal ions ($n = 28$)
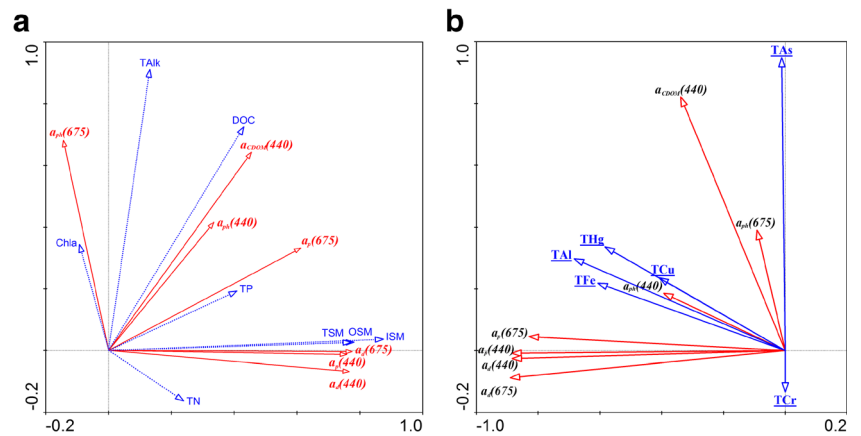
exhibited positive correlations with each other, while a negative correlation was obtained between TAs and TCr. Coefficients between metal ions with axes in the RDA indicated that TCu and THg had strong correlations with $a_p(440)$, $a_p(675)$, $a_{NAP}(440)$, and $a_{NAP}(675)$ (Table 6), while TAs were significantly correlated with $a_{CDOM}(440)$, and TAl was positively correlated with $a_p(675)$ and $a_{NAP}(675)$ ($p < 0.05$). Almost no correlation was found between phytoplankton absorption and the metal ions.

Discussion

Abundant terrigenous inorganic matter, such as suspended sediment, input into rivers was the main reason for the weak correlations between $a_p(\lambda)$ and Chla as shown in Table 5 and Fig. 5a. (Zhang et al. 2007a; Liu et al. 2011). Soil erosion, the liquidity of rivers themselves, and frequent sediment resuspension caused by strong windy conditions caused an increase in inorganic particulate matter and led to the increase in non-
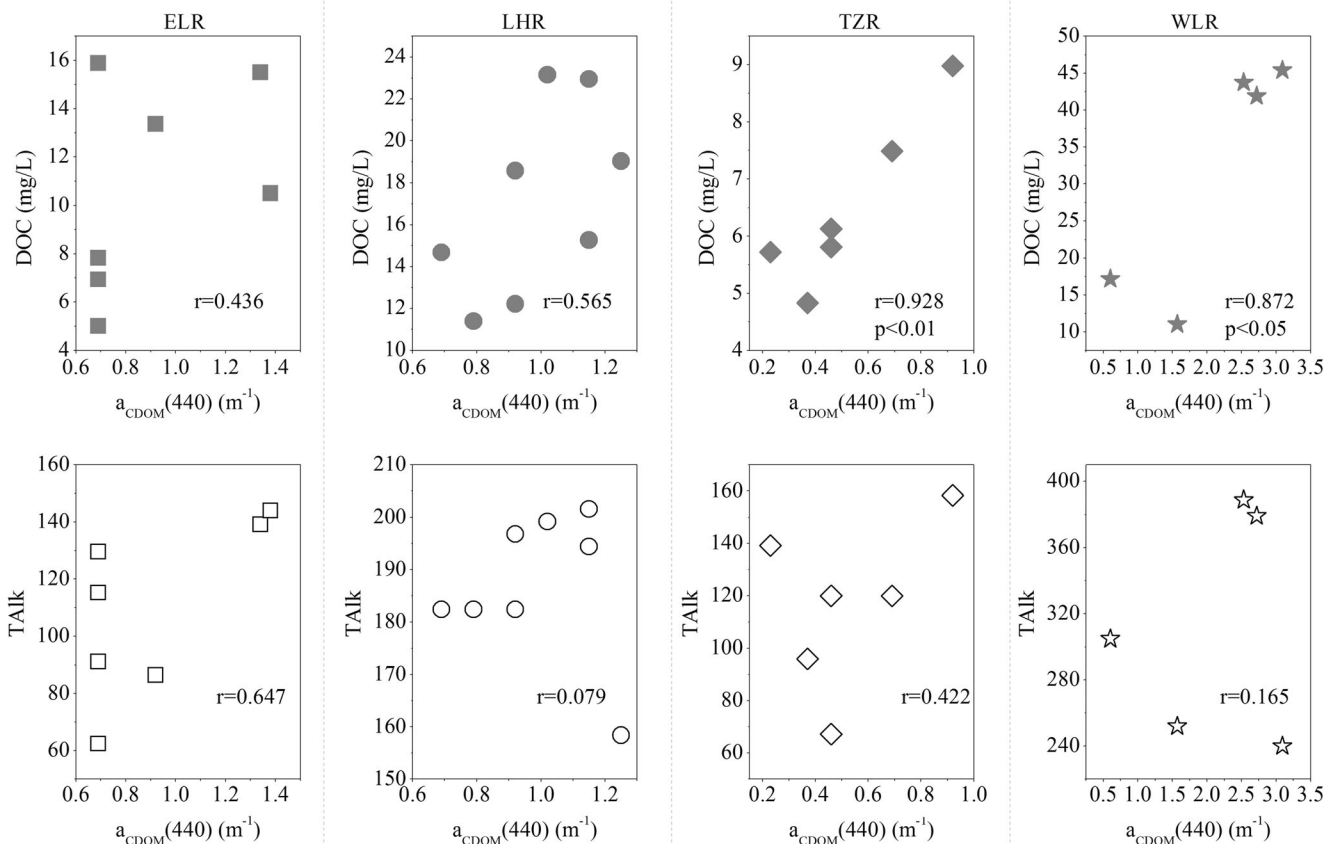
Fig. 6 Correlations between $a_{CDOM}(440)$ and DOC/TAlk for samples in different rivers

Table 6 Correlations between absorption and metal ion concentrations

| Ions	$a_p(440)$	$a_p(675)$	$a_d(440)$	$a_d(675)$	$a_{ph}(440)$	$a_{ph}(675)$	$a_{CDOM}(440)$	DOC	TAl	TFe	TCr	TCu	TAs	THg
TAl	0.367	0.461*	0.362	0.421*	0.151	0.188	0.238	0.294	1					
TFe	0.283	0.401*	0.280	0.351	0.104	0.213	0.197	0.223	0.916**	1				
TCr	−0.151	−0.166	−0.140	−0.176	−0.151	0.016	−0.287	−0.311	0.191	0.123	1			
TCu	0.431*	0.456*	0.429*	0.457*	0.136	0.048	0.310	0.426	0.496**	0.276	0.134	1		
TAs	−0.159	−0.023	−0.168	−0.109	0.045	0.288	0.910**	0.897**	0.080	0.064	−0.323	0.248	1	
THg	0.565**	0.512**	0.555**	0.554**	0.251	−0.088	0.464*	0.607**	−0.023	−0.225	−0.238	0.512**	0.439*	1

The unit of absorption coefficients is m^{-1}. The unit of TAl, TFe, TCu, and TCr is mg/L. The unit of TAs and THg is μg/L

**Correlation is significant at the 0.01 level (two-tailed); *correlation is significant at the 0.05 level (two-tailed)

algal absorption (Schallenberg and Burns 2004; Zhang et al. 2007a).

Previous studies claimed that the degradation of phytoplankton was the main process in the generation of non-algal particles for class I water, leading to the significant relationship between $a_{NAP}(\lambda)$ and Chla concentration (Cleveland 1995; Bricaud et al. 1998; Cao et al. 2003). In contrast, no correlations between $a_{NAP}(\lambda)$ and Chla were found in this study. Moreover, no correlation between Chla and $a_{ph}(\lambda)$ was obtained for water samples in the LHW (Fig. 7), which was quite different from the other class II waters. Previous studies on class II water bodies, such as estuaries, large lakes, and littoral belts, all showed strong correlations between the absorption coefficients of phytoplankton and the Chla concentrations (Gallegos 2005; Zhang et al. 2007a; Cao et al. 2003). The great variation in $a_{ph}(440)/a_{ph}(675)$ observed in this study demonstrated that Chla concentration in ELR, TZR, and WLR accounted for a smaller proportion of pigments than that in HHR and LHR. The $a_{ph}(440)$ was jointly determined by Chla and auxiliary pigments. As a result, different proportions of Chla in different rivers may be one reason leading to the relationship between Chla and $a_{ph}(440)$. Rivers are flowing waters and are very sensitive to the surrounding environment including land use/cover change in surrounding landscapes, human activities, agricultural tillage, precipitation, and other factors (Park et al. 2007; Piirsoo et al. 2012; Catalan et al. 2013; Le et al. 2015). As mentioned above, 28 groups of water samples were collected during the first field campaign, and data from two sampling sites (Xilamulun and Laoha rivers located in WLR) used in this study were collected in October. It is clear that $a_{ph}(675)$ of the two samples was much higher than that of the other water samples shown in Fig. 7. If the two samples collected in October were eliminated, significant correlation ($r = 0.61$, $p < 0.01$) was obtained between $a_{ph}(675)$ and Chla (Fig. 7). This pattern might be ascribed to two factors: (i) the locations of these two samples were in the Inner Mongolia autonomous region and far away from the other sampling sites (Fig. 1). Low precipitation and serious soil erosion in the WLR sub-catchments might be responsible for the inconsistency of synchronous changes in Chla

concentration with the other areas, and (ii) sampling time might be another explanation. During the two field campaigns, the growth status of algal particles gradually changed. Moreover, the two measurements of Chla and algal absorption might also show little difference. However, further research should be undertaken to identify the reasons for the discrepancy.

Significant positive correlations were shown between TSM, OSM, ISM, and particle and non-algal particle absorption (Table 5). In contrast, there were weak correlations between TSM, OSM, ISM, and $a_{ph}(440)$, and no correlations with $a_{ph}(675)$. Previous studies confirmed that the concentration of inorganic nutrients was high and nutrient amendments had often failed to stimulate the growth of phytoplankton (Paerl et al. 1983). The percentage of OSM determined the correlation between TSM, OSM, ISM, and Chla (Zhang et al. 2007a). In the case of the LHW, the percentage of ISM was much higher than that of OSM in all samples, suggesting that the concentration of OSM is the determining factor in the correlation with phytoplankton absorption.
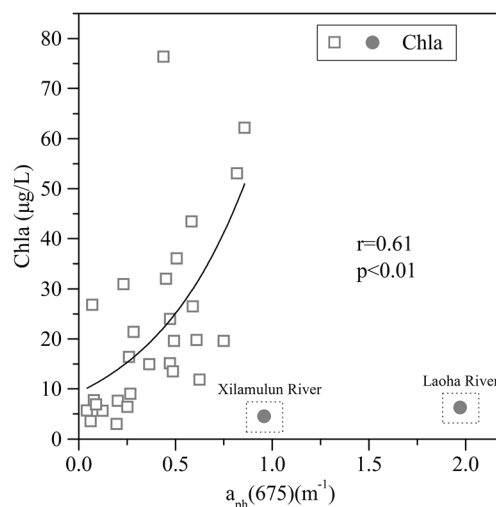
Fig. 7 Relationship between chlorophyll a (Chla) and the absorption coefficients of phytoplankton [$a_{ph}(\lambda)$]. After remove data at Xilamulun and Laoha rivers, the fitting curve was observed with $r = 0.61$

The absorption of light by CDOM can be explained by variations in nutrients and DOC concentration especially for $a_{CDOM}(440)$, which showed strong positive correlations with TN, TAlk, and DOC concentrations in all water samples. The present study has shown that strong relationships exist between DOC concentration and CDOM absorption in riverine waters, which is in agreement with several other studies (Seritti et al. 1998; Laurion et al. 2000; Spencer et al. 2012; Wen et al. 2016). However, not every river exhibited a strong correlation for the two parameters (Fig. 6). Two reasons might explain this result. First, the location of sampling sites in different rivers exhibited great variability. Samples from WLR were more scattered, while samples in ELR and LHR were more intensive, leading to the concentration gradients of CDOM and DOC to some extent. Second, the LHR passes through several big cities, which are associated with a large amount of polluted and wastewater with high CDOM concentrations, making it very different from the other rivers.

There were significant positive correlations between TAlk and CDOM obtained for the rivers within the LHW, which were seriously influenced by industrial and agricultural activities. Correlation between TAlk and CDOM absorption depends on the positive correlation of partial pressure of carbon dioxide (pCO$_2$) and CDOM that was observed in all systems (Clark et al. 2004; Else et al. 2008; Song et al. 2016). High CO$_2$ saturation has been attributed to high alkalinity in river inputs to coastal waters (Frankignoulle et al. 1996). Moreover, a river plume with high TAlk and hence higher bicarbonate concentrations would be expected to have higher pCO$_2$ levels (Clark et al. 2004). TAlk in rivers partly comes from effluents and detergent from papermaking, printing, and dyeing, as well as runoff of chemical fertilizers and pesticides, while pollution also raises CDOM concentration. Phosphate and nitrate are consumed during primary production, leading to reductions in TAlk and CO$_2$ and resulting in decreased pCO$_2$ in the water column, while microbial respiration increases CO$_2$ (Packard et al. 1996; Clark et al. 2004). If other influencing factors are eliminated, the stronger the photosynthesis by phytoplankton, the lower TAlk will be. The significant positive correlation between $a_{ph}(675)$ and TAlk suggested that phytoplankton photosynthesis was not the main factor controlling the relationship with TAlk for rivers in the LHW.

Numerous studies have confirmed that strong relationships between THg and DOC exist in stream water (Driscoll et al. 1995; Selvendiran et al. 2008; Dittman et al. 2009); the same results were obtained for THg and DOC as well as CDOM in this investigation. Significant positive correlations between THg and absorptions of optically active substances implied that THg in the streams of the LHW affected the attenuation of solar ultraviolet radiation (UR) and water color (Maloney et al. 2005). No strong correlation between TFe and CDOM was obtained for the samples in the LHW, which is inconsistent with other studies that found that TFe was highly correlated with

water color and when in complexation with organic compounds absorbs light in the UV range (Heikkinen and Ihme 1995; Maloney et al. 2005; Xiao et al. 2013). There were two reasons to explain this difference. One is that previous studies obtained TFe concentrations at different depths, while the samples in this study were obtained only 0.1 m below the river surface. The other reason is that significant correlations were generally acquired in humic waters (Schelker et al. 2011), where humic substances and Fe interacted to form complexes allowing Fe to remain in solution, whereas the rivers in the LHW were not typical humic rivers. TAs and THg showed positive correlations with both CDOM and DOC, especially TAs. Fulvic or humic acids can form stable complexes on mineral surfaces (Kaiser et al. 1997) effectively blocking arsenic from adsorption on iron ($r = 0.064$), alumina ($r = 0.080$), quartz, or kaolinite (Grafe et al. 2001; Grafe et al. 2002; Xu et al. 1991), leading to a strong correlation between arsenic and CDOM/DOC. Moreover, previous studies confirmed that the band ratio B_{711}/B_{406} had high correlation with Cu ($r = 0.749$) for the Pearl River estuary based on in situ measured remote sensing reflectance and EO-1 Hyperion images (Chen et al. 2010), while other investigators demonstrated that complexes formed by heavy metals and humic substances/organic matter strongly affected metal bioavailability and were an important component in influencing the light absorption of water (Ortega-Retuerta et al. 2010; Xiao et al. 2013; Zhang et al. 2014). As a result, significant correlations between heavy metals and the light absorption of CDOM and particulates in LHW signified manifested significant influence of metals on the characteristics of optically active substances and the absorption of solar UR.

While the present study provided a detailed description on the spectral absorption characteristics of optically active substances and determined the factors impacting the absorption coefficients, it was not designed to study the mechanism between absorption characteristics and water quality parameters. Moreover, water samples used in this study were collected only from late September to early October and are not sufficient to address the seasonal changes and transformations of absorption characteristics of optically active substances and the interaction between absorption and water parameters from headstreams to the estuaries for the Liaohe River system. Additional research is needed to study the mechanism and interaction between absorption and environmental factors and to address how the absorption of optically active substances affects light attenuation in rivers.

Conclusions

The LHR watershed is an important agricultural region but also includes some of the most heavily industrialized areas of China. While these intensive forms of land use have spurred economic development, they have also led to serious water

problems. A preliminary study was conducted to present an overall view of absorption characteristics of optically active constituents and to provide insight into particulates and CDOM properties linked to water quality characteristics in LRS that is seriously influenced by anthropogenic and natural factors. The absorption coefficient of CDOM is similar to that of non-algal particle absorption. When S_g values in the LHW were compared with rivers in other regions, the molecular weight of CDOM composition in the LHW was higher than in the Changjiang, Suwannee, and Elizabeth rivers, while it was lower than in rivers located at high latitude. The relative contribution of non-algal particle absorption was higher than the other constituents for most samples, implying the crucial role of non-algal particles to light attenuation in rivers. TSM, OSM, and ISM were strongly correlated with $a_p(440)$ and $a_p(675)$ ($p < 0.01$), while DOC showed weak correlations with particle absorption. Furthermore, $a_{CDOM}(440)$ exhibited significant correlations with DOC and TAlk ($p < 0.01$). There was almost no correlation between the absorption of total suspended particles and Chla, TN, TP, and TAlk. Significant correlation was observed between $a_{ph}(675)$ and Chla after eliminating two samples collected in October. Moreover, TCu and THg were strongly correlated with $a_p(440)$, $a_p(675)$, $a_d(440)$, and $a_d(675)$. TAs showed a significant correlation with $a_{CDOM}(440)$, and positive correlations between TAl and $a_p(675)$ and $a_d(675)$ ($p < 0.05$) were obtained. This study on optical–physicochemical correlation will contribute to bio-optical models and is helpful for understanding the interaction between optically active substances and heavy metals in river water environments.

References

Anawar HM, Akai J, Komaki K et al (2003) Geochemical occurrence of arsenic in groundwater of Bangladesh: sources and mobilization processes. J Geochem Explor 77(2):109–131

Babin M, Stramski D, Ferrari GM, et al. (2003) Variations in the light absorption coefficients of phytoplankton, nonalgal particles, and dissolved organic matter in coastal waters around Europe. J Geophys Res Oceans 108(C7)

Binding CE, Bowers DG, Mitchelson-Jacob EG (2005) Estimating suspended sediment concentrations from ocean colour measurements in moderately turbid waters; the impact of variable particle scattering properties. Remote Sens Environ 94(3):373–383

Binding CE, Jerome JH, Bukata RP et al (2008) Spectral absorption properties of dissolved and particulate matter in Lake Erie. Remote Sens Environ 112(4):1702–1711

Bracchini L, Tognazzi A, Dattilo AM et al (2010) Sensitivity analysis of CDOM spectral slope in artificial and natural samples: an application in the central eastern Mediterranean Basin. Aquat Sci 72(4):485–498

Bricaud A, Morel A, Prieur L (1981) Absorption by dissolved organic matter of the sea (yellow substance) in the UV and visible domains. Limnol Oceanogr 26(1):43–53

Bricaud A, Morel A, Babin M et al (1998) Variations of light absorption by suspended particles with chlorophyll a concentration in oceanic (case 1) waters—analysis and implications for bio-optical models. J Geophys Res 103(C13):31033–31044

Cao W, Yang Y, Xu X et al (2003) Regional patterns of particulate spectral absorption in the Pearl River estuary (in Chinese with English abstract). Chin Sci Bull 48(21):2344–2351

Catalán N, Obrador B, Alomar C et al (2013) Seasonality and landscape factors drive dissolved organic matter properties in Mediterranean ephemeral washes. Biogeochemistry 112(1–3):261–274

Chen CQ, Liu F, He Q, et al. (2010) The possibility on estimation of concentration of heavy metals in coastal waters from remote sensing data[C]//Geoscience and Remote Sensing Symposium (IGARSS), 2010 I.E. International. IEEE 4216–4219

Chen H, Meng W, Zheng B et al (2013) Optical signatures of dissolved organic matter in the watershed of a globally large river (Yangtze River, China). Limnologica-Ecol Manag Inland Waters 43(6):482–491

Clark CD, Hiscock WT, Millero FJ et al (2004) CDOM distribution and CO_2 production on the Southwest Florida Shelf. Mar Chem 89(1):145–167

Cleveland JS (1995) Regional models for phytoplankton absorption as a function of chlorophyll a concentration. J Geophys Res : Oceans 100(C7):13333–13344

Del Castillo CE, Miller RL (2008) On the use of ocean color remote sensing to measure the transport of dissolved organic carbon by the Mississippi River Plume. Remote Sens Environ 112(3):836–844

Dittman JA, Shanley JB, Driscoll CT et al (2009) Ultraviolet absorbance as a proxy for total dissolved mercury in streams. Environ Pollut 157(6):1953–1956

Driscoll CT, Blette V, Yan C, et al. (1995) The role of dissolved organic carbon in the chemistry and bioavailability of mercury in remote Adirondack lakes[M]//mercury as a global pollutant. Springer Netherlands 499–508

Else BGT, Yackel JJ, Papakyriakou TN (2008) Application of satellite remote sensing techniques for estimating air-sea CO_2 fluxes in Hudson Bay, Canada during the ice-free season. Remote Sens Environ 112(9):3550–3562

Estapa ML, Boss E, Mayer LM et al (2012) Role of iron and organic carbon in mass-specific light absorption by particulate matter from Louisiana coastal waters. Limnol Oceanogr 57(1):97–112

Fichot CG, Benner R (2011) A novel method to estimate DOC concentrations from CDOM absorption coefficients in coastal waters. Geophys Res Lett 38(3)

Frankignoulle M, Bourge I, Canon C et al (1996) Distribution of surface seawater partial CO_2 pressure in the English Channel and in the Southern Bight of the North Sea. Cont Shelf Res 16(3):381–395

Gallegos CL (2005) Optical water quality of a blackwater river estuary: the Lower St. Johns River, Florida, USA. Estuar Coast Shelf Sci 63(1):57–72

Gao J, Yang H, Li B (2016) Investigating the roles of dissolved organic matter on arsenic mobilization and speciation in environmental water. CLEAN Soil Air Water 44(7):818–828

Gonnelli M, Vestri S, Santinelli C (2013) Chromophoric dissolved organic matter and microbial enzymatic activity. A biophysical approach to understand the marine carbon cycle. Biophys Chem 182:79–85

Grafe M, Eick MJ, Grossl PR (2001) Adsorption of arsenate (V) and arsenite (III) on goethite in the presence and absence of dissolved organic carbon. Soil Sci Soc Am J 65(6):1680–1687

Grafe M, Eick MJ, Grossl PR et al (2002) Adsorption of arsenate and arsenite on ferrihydrite in the presence and absence of dissolved organic carbon. J Environ Qual 31(4):1115–1123

Heikkinen K, Ihme R (1995) Retention of organic Fe-P-colloids from peat mining water in an overland flow wetland treatment system in northern Finland. Archiv Hydrobiol 134(4):547–560

Helms JR, Stubbins A, Ritchie JD et al (2008) Absorption spectral slopes and slope ratios as indicators of molecular weight, source, and photobleaching of chromophoric dissolved organic matter. Limnol Oceanogr 53(3):955–969

Hestir EL, Brando V, Campbell G et al (2015) The relationship between dissolved organic matter absorption and dissolved organic carbon in reservoirs along a temperate to tropical gradient. Remote Sens Environ 156:395–402

Kaiser K, Guggenberger G, Haumaier L et al (1997) Dissolved organic matter sorption on sub soils and minerals studied by 13C-NMR and DRIFT spectroscopy. Eur J Soil Sci 48(2):301–310

Kalbitz K, Wennrich R (1998) Mobilization of heavy metals and arsenic in polluted wetland soils and its dependence on dissolved organic matter. Sci Total Environ 209(1):27–39

Kalenak D, Boss E, Effler SW (2013) Inherent optical properties of suspended particulates in four temperate lakes: application of in situ spectroscopy. Hydrobiologia 713(1):127–148

Kitidis V, Stubbins AP, Uher G et al (2006) Variability of chromophoric organic matter in surface waters of the Atlantic Ocean. Deep-Sea Res II Top Stud Oceanogr 53(14):1666–1684

Laurion I, Ventura M, Catalan J et al (2000) Attenuation of ultraviolet radiation in mountain lakes: factors controlling the among- and within-lake variability. Limnol Oceanogr 45(6):1274–1288

Le CF, Lehrter JC, Hu CM et al (2015) Relation between inherent optical properties and land use and land cover across Gulf Coast estuaries. Limnol Oceanogr 60(3):920–933

Lepš J, Šmilauer P (2003) Multivariate analysis of ecological data using CANOCO[M]. Cambridge university press

Li LH, Li L, Song K et al (2013) An inversion model for deriving inherent optical properties of inland waters: establishment, validation and application. Remote Sens Environ 135:150–166

Liu CX, Guo ZQ, Zhang BG et al (2011) Absorption characteristics of particulates and the CDOM in spring in Lake Kuncheng, Taihu Basin (in Chinese with English abstract). J Lake Sci 23(5):773–782

Long CM, Pavelsky TM (2013) Remote sensing of suspended sediment concentration and hydrologic connectivity in a complex wetland environment. Remote Sens Environ 129:197–209

Ma RH, Tang J, Dai J et al (2006) Absorption and scattering properties of water body in Taihu Lake, China: absorption. Int J Remote Sens 27(19):4277–4304

Maloney KO, Morris DP, Moses CO et al (2005) The role of iron and dissolved organic carbon in the absorption of ultraviolet radiation in humic lake water. Biogeochemistry 75(3):393–407

Niu C, Zhang Y, Zhou Y et al (2014) The potential applications of real-time monitoring of water quality in a large shallow lake (Lake Taihu, China) using a chromophoric dissolved organic matter fluorescence sensor. Sensors 14(7):11580–11594

Organelli E, Bricaud A, Antoine D et al (2014) Seasonal dynamics of light absorption by chromophoric dissolved organic matter (CDOM) in the NW Mediterranean Sea (BOUSSOLE site). Deep-Sea Res I Oceanogr Res Pap 91:72–85

Ortega-Retuerta E, Reche I, Pulido-Villena E et al (2010) Distribution and photoreactivity of chromophoric dissolved organic matter in the Antarctic Peninsula (Southern Ocean). Mar Chem 118(3):129–139

Osburn CL, Wigdahl CR, Fritz SC et al (2011) Dissolved organic matter composition and photoreactivity in prairie lakes of the US Great Plains. Limnol Oceanogr 56(6):2371–2390

Packard T, Berdalet E, Blasco D et al (1996) CO_2 production predicted from isocitrate dehydrogenase activity and bisubstrate enzyme kinetics in the marine bacterium Pseudomonas nautica. Aquat Microb Ecol 11(1):11–19

Paerl HW, Tucker J, Bland PT (1983) Carotenoid enhancement and its role in maintaining blue-green algal (Microcystis aeruginosa) surface blooms. Limnol Oceanogr 28(5):847–857

Park JH, Lee JH, Kang SY et al (2007) Hydroclimatic controls on dissolved organic matter (DOM) characteristics and implications for trace metal transport in Hwangryong River Watershed, Korea, during a summer monsoon period. Hydrol Process 21(22):3025–3034

Phong DD, Lee Y, Shin KH et al (2014) Spatial variability in chromophoric dissolved organic matter for an artificial coastal lake (Shiwha) and the upstream catchments at two different seasons. Environ Sci Pollut Res 21(12):7678–7688

Piirsoo K, Viik M, Kõiv T et al (2012) Characteristics of dissolved organic matter in the inflows and in the outflow of Lake Võrtsjärv, Estonia. J Hydrol 475:306–313

Schallenberg M, Burns CW (2004) Effects of sediment resuspension on phytoplankton production: teasing apart the influences of light, nutrients and algal entrainment. Freshw Biol 49(2):143–159

Schelker J, Burns DA, Weiler M, et al. (2011) Hydrological mobilization of mercury and dissolved organic carbon in a snow-dominated, forested watershed: conceptualization and modeling. J Geophys Res : Biogeosci 116(G1)

Schuster PF, Shanley JB, Marvin-Dipasquale M et al (2008) Mercury and organic carbon dynamics during runoff episodes from a northeastern USA watershed. Water Air Soil Pollut 187(1–4):89–108

Selvendiran P, Driscoll CT, Bushey JT et al (2008) Wetland influence on mercury fate and transport in a temperate forested watershed. Environ Pollut 154(1):46–55

Seritti A, Russo D, Nannicini L et al (1998) DOC, absorption and fluorescence properties of estuarine and coastal waters of the Northern Tyrrhenian Sea. Chem Speciat Bioavailab 10(3):95–106

Shao TT, Song KS, Du J et al (2016) Seasonal variations of CDOM optical properties in rivers across the Liaohe Delta. Wetlands 36(1):181–192

Shen Y, Fichot CG, Benner R (2012) Floodplain influence on dissolved organic matter composition and export from the Mississippi-Atchafalaya River system to the Gulf of Mexico. Limnol Oceanogr 57(4):1149–1160

Siegel DA, Maritorena S, Nelson NB, et al (2005) Independence and interdependencies among global ocean color properties: reassessing the bio-optical assumption. J Geophys Res : Oceans 110(C7)

Song KS, Lu DM, Li L et al (2012) Remote sensing of chlorophyll-a concentration for drinking water source using genetic algorithms (GA)-partial least square (PLS) modeling. Ecol Inform 10:25–36

Song KS, Li L, Tedesco LP et al (2013) Remote estimation of chlorophyll-a in turbid inland waters: three-band model versus GA-PLS model. Remote Sens Environ 136:342–357

Song X, Bai Y, Cai WJ et al (2016) Remote sensing of sea surface pCO_2 in the Bering Sea in summer based on a mechanistic semi-analytical algorithm (MeSAA). Remote Sens 8(7):558

Spencer RGM, Aiken GR, Butler KD, et al. (2009) Utilizing chromophoric dissolved organic matter measurements to derive export and reactivity of dissolved organic carbon exported to the Arctic Ocean: a case study of the Yukon River, Alaska. Geophys Res Lett 36(6)

Spencer RGM, Butler KD, Aiken GR (2012) Dissolved organic carbon and chromophoric dissolved organic matter properties of rivers in the USA. J Geophys Research: Biogeosci 117(G3)

Stramski D, Woźniak SB, Flatau PJ (2004) Optical properties of Asian mineral dust suspended in seawater. Limnol Oceanogr 49(3):749–755

Tilstone GH, Smyth TJ, Gowen RJ et al (2005) Inherent optical properties of the Irish Sea and their effect on satellite primary production algorithms. J Plankton Res 27(11):1127–1148

Vähätalo AV, Wetzel RG, Paerl HW (2005) Light absorption by phytoplankton and chromophoric dissolved organic matter in the drainage

basin and estuary of the Neuse River, North Carolina (USA). Freshw Biol 50(3):477–493

Wang Y, Zhang D, Shen Z et al (2014) Characterization and spacial distribution variability of chromophoric dissolved organic matter (CDOM) in the Yangtze Estuary. Chemosphere 95:353–362

Wen ZD, Song KS, Zhao Y et al (2016) Influence of environmental factors on spectral characteristics of chromophoric dissolved organic matter (CDOM) in Inner Mongolia Plateau, China. Hydrol Earth Syst Sci 20(2):787–801

Xiao YH, Sara-Aho T, Hartikainen H et al (2013) Contribution of ferric iron to light absorption by chromophoric dissolved organic matter. Limnol Oceanogr 58(2):653–662

Xu H, Allard B, Grimvall A (1991) Effects of acidification and natural organic materials on the mobility of arsenic in the environment. Water Air Soil Pollut 57(1):269–278

Zhang YL, Qin BQ, Zhang L et al (2005) Spectral absorption and fluorescence of chromophoric dissolved organic matter in shallow lakes in the middle and lower reaches of the Yangtze River. J Freshw Ecol 20(3):451–459

Zhang YL, Zhang B, Wang X et al (2007a) A study of absorption characteristics of chromophoric dissolved organic matter and particles in Lake Taihu, China. Hydrobiologia 592(1):105–120

Zhang YL, Qin BQ, Zhu G et al (2007b) Chromophoric dissolved organic matter (CDOM) absorption characteristics in relation to fluorescence in Lake Taihu, China, a large shallow subtropical lake. Hydrobiologia 581(1):43–52

Zhang YL, van Dijk MA, Liu ML et al (2009) The contribution of phytoplankton degradation to chromophoric dissolved organic matter (CDOM) in eutrophic shallow lakes: field and experimental evidence. Water Res 43(18):4685–4697

Zhang Y, Zhang Y, Yu T (2014) Quantitative characterization of Cu binding potential of dissolved organic matter (DOM) in sediment from Taihu Lake using multiple techniques. Front Environ Sci Eng 8(5):666–674